JMATPRO

Journal of Advanced Materials and Processing
10 (2): 39-46, Spring 2022
http://jmatpro.iaun.iau.ir
20.1001.1.2322388.2022.10.2.5.0

Research Paper

The Effects of Oxide Fluxes on the Penetration Depth of 316L and A516 Steels in A-TIG Welding: a Comparative Study

Mohammad Emami[1], Seyed Hossein Elahi[2*]

1 Assistant Professor, Department of Materials Science and Engineering, University of Bonab, Bonab, Iran.
2 Assistant Professor, Department of Mechanical engineering, Arak University of Technology, Arak, Iran.

ARTICLE INFO

Article history:

Received 3 February 2022
Accepted 17 March 2022
Available online 1 April 2022

Keywords:
A-TIG
Oxide flux
Viscosity
Surface tension
Reverse Marangoni

ABSTRACT

The present work evaluates the mechanisms that cause the weld geometry to change in activating flux TIG (A-TIG) welding. For this purpose, an austenitic 316 stainless steel and ferritic A516 steel in conventional TIG and A-TIG welding were compared and evaluated under the same process parameters. Al_2O_3, Fe_2O_3, MnO_2, SiO_2, and TiO_2 powders were used as activating fluxes. The depth of penetration and width of the beads were measured metallographically. In conventional TIG, the welds of carbon steel and stainless steel had a thickness of about 2.2 mm and 1.7 mm, respectively. A-TIG welding of 316 SS using TiO_2, MnO_2, and Fe_2O_3 led to a 75% increase in the weld depth. In the case of Al_2O_3 and SiO_2 the weld depth increased 50% and 9%, respectively. However, in A516 steel, less thermodynamically stable oxide fluxes such as MnO_2, and Fe_2O_3 had a smaller effect i.e., 9-22% increases. More stable oxides like Al_2O_3, SiO_2, and TiO_2 caused a decrease of about 30% in the weld depth compared to the conventional TIG weld. It was proposed that when the penetration increases, reverse Marangoni is dominant. This mechanism is mainly associated with viscosity and surface tension that vary by the dissolution of oxygen in the melt. Regarding penetration reduction, as in the case of more stable oxides like SiO_2, the energy dissipation by the flux through heating and dissociation of the oxide and barrier effect of the undissolved oxide dominate.

Citation: Emami, M.; Elahi, S.H. (2022). The Effects of Oxide Fluxes on the Penetration Depth of 316L and A516 Steels in A-TIG Welding: a Comparative Study, Journal of Advanced Materials and Processing, 10 (2), 39-46. Dor: 20.1001.1.2322388.2022.10.2.5.0

[*] **Corresponding Author**
E-mail Address: h.elahi@arakut.ac.ir

1. Introduction

TIG welding is a popular method for joining ferrous and non-ferrous alloys [1]. High-quality and clean welds, good surface finish, and inexpensive equipment are some of the advantages of this technique [1]. The low deposition rate and productivity of TIG welds have restricted the application of this method to thin sections, which is the reason for its slow growth rate in the industry [2]. Enhancing the penetration of TIG welding could compensate for the low deposition rate. A thin layer of oxide or fluoride fluxes could enhance the penetration depth of the welds. The process is known as active flux TIG, or A-TIG, and was introduced by Paton Electric Welding Institute in the 1960s [3, 4]. The flux increases the penetration by contracting the arc and reversing the Marangoni convection. Li et al. [5] investigated the effect of oxygen directly blown to the weld pool through a double-shielded TIG method on the shape of the weld pool. Oxygen caused a deeper weld pool compared to TIG welding [5]. Double-shielded (Ar + CO_2) TIG welding of carbon steel also confirmed that certain amounts of oxygen from decomposing of CO_2, could increase the penetration depth [6]. Small additions of SO2 in argon shielding gas improved joint penetration [7]. The addition of small amounts of sulfur and selenium, tolerable by the base metal, could enhance TIG penetration [8, 9]. The considerable effect of MWCNT-TiO_2 flux on the penetration depth of 6061 aluminum was confirmed by Muzamil et al. [2]. Ramkumar et al. [10] reported that both SiO_2 and Fe_2O_3 fluxes improved the weld depth in SS430 and made 5 mm-thick welds accessible in a single pass. The effects of Cu_2O, NiO, Cr_2O_3, SiO_2, and TiO_2 fluxes on the penetration depth of SS304 TIG welds were investigated by Lu et al. [11]. Yushchenko et al. [12] did experimental and mathematical investigations on the electromagnetic and hydrodynamic processes occurring in the weld pool of SS304 in TIG and A-TIG welding and found a good agreement between experimental and calculated results. The comparison of mono- and multi-component oxide fluxes on the TIG welding of stainless steels was reported in [1, 13, 14]. A mixture of MnO_2 and ZnO fluxes led to full penetration in 5 mm-thick SS304 sheets [15]. Several mechanisms were proposed for the higher penetration associated with activating fluxes, two of which are commonly accepted: reverse Marangoni and arc constriction [16-18]. The former is attributed to the reduction of the surface tension at the center of the weld pool under the influence of oxygen and the resulting convection from the periphery to the center of the pool. The latter refers to the reduction of the plasma arc diameter while moving from the bare to the flux-coated surface. The reduced arc diameter leads to an increased current density and, therefore, a narrower and deeper weld. Buoyancy forces, electromagnetic forces, and aerodynamic forces are less common mechanisms proposed in the literature [19].

A-TIG has principally been known to increase the penetration depth of the welds. Nonetheless, in some circumstances, fluxes could lower the weld penetration, which has been disregarded in the research works. Moreover, researchers disagree on a single depth-enhancing mechanism in A-TIG welding. Hence, in this paper, two objectives are pursued: first, to determine the dominant mechanisms responsible for increasing the penetration depth in A-TIG welding. Second, to explain factors that may render the A-TIG process less efficient. Hence, the effects of various oxide fluxes on the penetration depth of SS316 and A516 ferritic steel with different thermophysical properties were studied. The results were compared with the preceding works, and some mechanisms were proposed following a comprehensive discussion.

2. Experimental procedure

Plates of SS316L and A516 Grade 70 steel with dimensions of 80mm ×40mm ×8mm were used, and the chemical compositions are shown in Table 1. The chemical composition and trace elements, such as sulfur, can have a great impact on weld penetration [9]. In order for the chemical composition to be as constant as possible, all tests were performed on a small piece of steel. Bead-on-plate welding was performed to avoid any discrepancies caused by edge preparation and fitting of the sample. Five different oxide powders of Fe_2O_3, Al_2O_3, SiO_2, TiO_2, and MnO_2 with a purity of 99.5% were used. The oxide powder was added to the acetone and then mixed using a mechanical stirrer to obtain a homogeneous activating agent. A thin layer of the flux with a thickness of about 0.2 mm and a width of 20 mm was applied on the specimens using a paintbrush. To obtain a reliable flux thickness, oxides were weighed using a 0.01 g balance following the calculations shown in Table 2. After the acetone was evaporated, a dry layer of flux remained on the surface.

Table 1. Chemical composition of the SS316L and A516 steel (in wt.%)

	Fe	**C**	**Mn**	**Si**	**P**	**S**	**Cr**	**Mo**	**Ni**	**N**
SS316L	Bal.	0.02	1.51	0.42	0.017	0.002	16.8	2.15	10.1	0.0
A516	Bal.	0.16	1.17	0.33	0.009	0.003	0.02	0.006	0.01	-

Single-pass TIG welding using a non-consumable thoriated tungsten electrode (diameter of 2.4 mm) was performed by employing a DCEN polarity power source at the current of 100 A, constant speed of 2 mm/s under high purity argon shielding with a flowrate of 12 L/min. To perform welding at a constant travel speed, a mechanized welding process was used. The angle of the electrode was 30°, and its tip was at a distance of 2 mm from the surface. To observe the arc shape, a camera was placed in front of the weld at a secure distance from the welding assembly. After the welding, the cross-section of the samples was prepared for macro-examination following the conventional metallographic procedure. The geometry (depth and width) of the welds was measured by a non-contact measuring system at a magnification of 8X.

Table 2. The calculations to obtain the required oxide mass for a flux of 0.2 mm thickness

Flux	Width (cm)	Length (cm)	Thickness (cm)	Density (g/cm^3)	Mass (g)
TiO_2	2	15	0.02	4.23	2.54
SiO_2	2	15	0.02	2.65	1.59
Al_2O_3	2	15	0.02	3.95	2.37
Fe_2O_3	2	15	0.02	5.24	3.14
MnO_2	2	15	0.02	5.03	3.02

3. Results and Discussion

The macrographs of the cross-sections of A516 samples welded with and without activating fluxes could be seen in Fig. 1. The MnO_2 and Fe_2O_3 flux-assisted welds (Figs. 1c, d) had depths comparable to that of the conventionally welded sample (Fig. 1a). But the welds obtained using TiO_2, SiO_2, and Al_2O_3 (Figs. 1b, e, and f) were shallower than the TIG weld. This means a negative and/or negligible effect of fluxes on the penetration depth of the carbon steel welds. These results contradict those obtained by Mirzaei et al. [6] and de Azevedo et al. [20] on A-TIG welding of ferritic steels. A wide heat-affected zone (HAZ) observed in A516 steel could be attributed to the large thermal conductivity of carbon steels [18].

The macrographs of the cross-sections of the SS316 specimens welded using TIG and A-TIG processes are shown in Fig. 2. It is seen that TIG welding of SS316 caused a shallow and wide weld pool. According to Fig. 2(b-f), various fluxes enhanced the penetration depth and reduced the width of the bead. Nonetheless, SiO_2 and to a lesser extent Al_2O_3 were less effective. Comparing Fig. 2a and Fig. 1a shows that the penetration depth of the original weld of A516 was greater than that of SS316. However, when the same fluxes were employed the penetration depth was reversed.

Fig. 3a makes a quantitative comparison of the penetration depth of A516 and SS316 welds using different fluxes. Fig. 3a shows that in the case of SS316, TIG welding led to the shallowest weld with 1.7 mm depth. TiO_2, MnO_2, and Fe_2O_3 caused about a 75% increase in the penetration depth of SS316. Al_2O_3 by about 50% increase was a little less effective. The least effective flux was SiO_2 with merely a 9% of depth increase. The penetration depths in this study were smaller than those reported by Tseng et al. [21] and Liu et al. [22] because they performed welding at a higher current and/or a lower speed which provided greater heat for deeper weld.

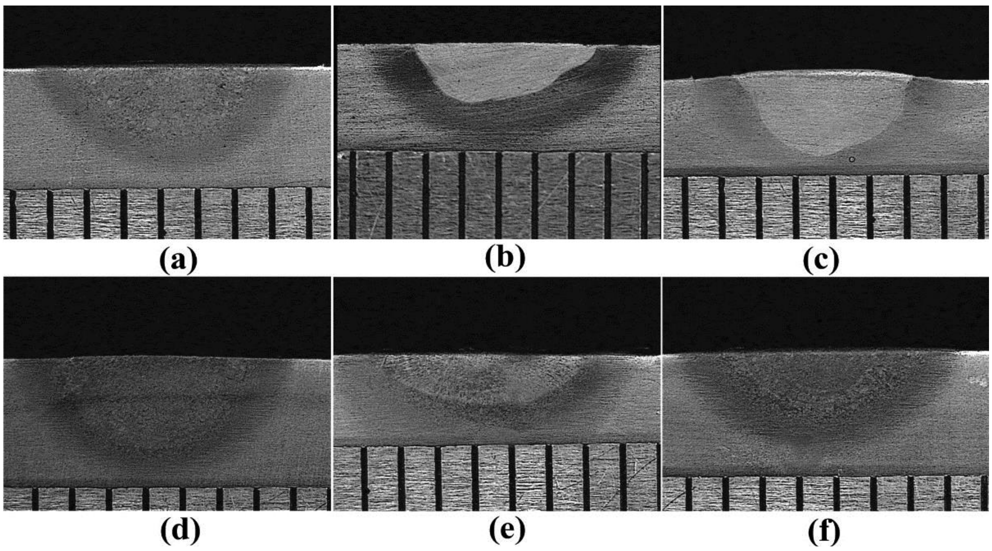

Fig. 1. Cross-sectional view of A516 welds welded a: without flux, b: with TiO_2 flux, c: with MnO_2 flux, d: with Fe_2O_3, e: with SiO_2 flux, and f: with Al_2O_3 flux.

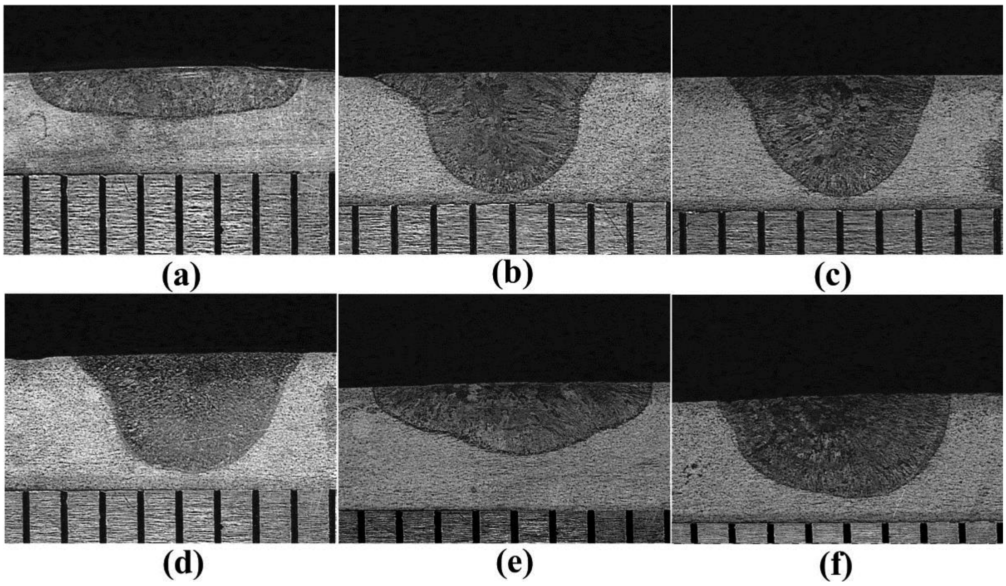

Fig. 2. Cross-sectional view of SS316 welds welded a: without flux, b: with TiO_2 flux, c: with MnO_2 flux, d: with Fe_2O_3 flux, e: with SiO_2 flux, and f: with Al_2O_3 flux.

In TIG welding of A516, a weld depth of 2.2 mm was obtained, about 30% higher than that of SS316. However, the depth of the flux-assisted welds decreased in the case of TiO_2, SiO_2, and Al_2O_3, and/or the increase was not significant when MnO_2 was employed. According to Fig. 1, the best result was attained when Fe_2O_3 was used. Similar results were obtained in studies of Tseng et al. [21] in A-TIG welding of SS316 and Dhandha and Badheka [23] in welding of P91 steel when stable oxides like Al_2O_3 and CaO were used. The effect of activating fluxes on the width of the bead of different specimens shown in Fig. 3b is quite straightforward. For both ferritic and austenitic steels, the weld bead narrowed down by applying fluxes, except SiO_2, which marginally got the weld widened.

Regarding TIG welding, a deeper weld was observed in A516 steel than in SS316 under the same welding parameters. The thermal conductivity and diffusivity of SS316 are lower than those of carbon steel. Thermal diffusivity is the thermal conductivity divided by density and specific heat capacity at constant pressure, suggesting that heat transfers slowly in a material with low thermal diffusivity. This may increase weld penetration by concentrating the arc energy. However, the viscosity of austenitic steels is lower than ferritic steels [24]. It was reported that an increase in the melt viscosity would result in a reduced weld penetration because high viscosity restricts the fluid flow [25, 26]. This means that in stainless steels, viscosity has a greater impact on weld penetration rather than thermal conductivity. It is noteworthy that, during heating, in stainless steel and carbon steel welds, the HAZ transforms to delta ferrite and austenite, respectively [27, 28]. This makes the heat transfer of these steels complicated. It was beyond the scope of this paper to measure the HAZ size of the welds, and no reliable data could be obtained from the macrographs shown in Figs. 1 and 2. However, it has been widely accepted and confirmed that under the same welding conditions, ferritic alloys show a wider HAZ than austenitic ones [29]. The bigger HAZ width in carbon steel indicates this alloy's higher conductivity. The other important point is the higher sulfur content of carbon steels in routine products, and sulfur could increase the weld penetration, which means the carbon steel with higher sulfur content already has an inherent active flux.

The results showed that SiO_2 and Al_2O_3 were less effective in enhancing the weld depth. A schematic representation in Fig. 4 compares the conventional TIG (Fig. 4a) with A-TIG in different conditions (Figs. 4b, c). According to Ellingham–Richardson diagram, SiO_2, TiO_2, and Al_2O_3 are the most stable oxides. To have a good penetration in the A-TIG process, the oxide flux should be dissociated and oxygen atoms should be dissolved in the melt. This happens more effectively in the less stable oxides. Moreover, the stoichiometry of the oxide may affect the amount of oxygen provided for the melt. Theoretically, oxides like MnO_2 and TiO_2 should be more effective than Al_2O_3. However, the weld penetration measurements showed an exception in the case of SiO_2. In more stable oxides, the arc temperature, especially at the colder peripheral zone, was insufficient to decompose the oxides. When the arc collides with stable oxides such as Al_2O_3 or SiO_2, the arc energy is not enough to decompose the flux, and the flux layer acts as a barrier against the arc. Thus, the arc is deviated from the straight path and spreads out toward the arc edges, which leads to an increased arc width. This mechanism can be schematically seen in Fig. 4c.

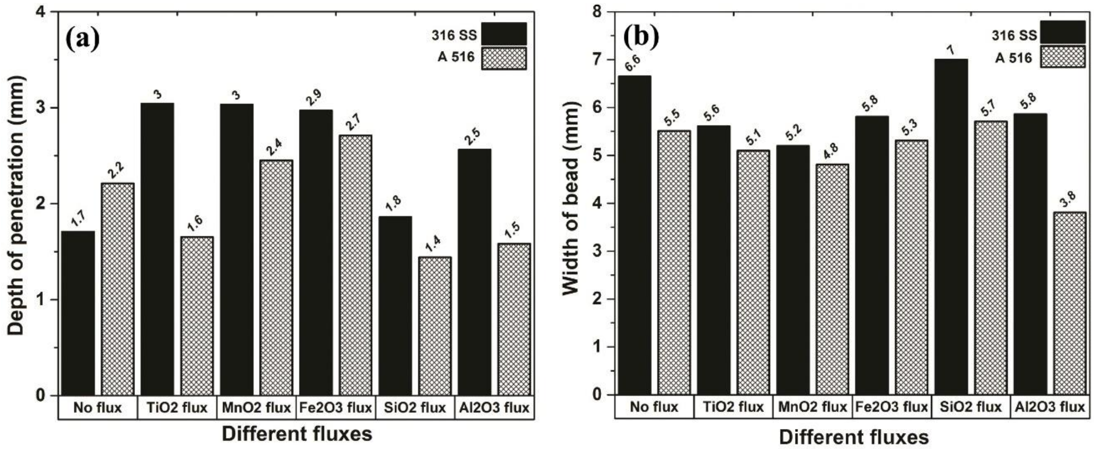

Fig. 3. a: Penetration depth of the welds with and without flux, b: width of the weld beads with and without flux.

In contrast, when the arc energy is able to overcome the flux layer, a small hole forms in the center of the flux due to a higher temperature in the middle of the arc. The metal underneath is directly exposed to the arc energy, and leads to increased metal evaporation, and the arc flare concentrates in the center of the weld pool [30, 31].

As stated earlier, the reverse effect of fluxes has been overlooked in the literature. When fluxes are used, the arc energy could be dissipated in some ways: consuming the arc energy by heating the fluxes, decomposition of the flux, and the barrier effect of the fluxes. Generally, the formation of an oxide layer on the surface of the weld pool reduces the weld penetration [6] and, more importantly, prevents the weld pool surface from moving freely and, therefore, inward Marangoni convection could be disturbed even if the oxide has a thickness lower than 50 μm [32] which is much thinner than the thickness of active fluxes. Also, when the heat input is insufficient to decompose the oxide flux, the fluid flow could get the oxide layer immersed in the melt pool as an inclusion. The formation of a dual-phase fluid (i.e., the melt and oxide inclusions), in turn, leads to a viscosity rise and a reduction in weld penetration [33, 34]. In brief, in A-TIG, two competing factors affect the weld penetration; the increase in the penetration by reversed Marangoni and arc constriction, and the reduction of the penetration by decreasing the arc force or dissipation of arc energy.

To verify the above arguments, MnO_2 as the most efficient flux was chosen for further study. A flux with a thickness of 0.5 mm (2.5 times thicker) was applied on SS316 and welding was performed using the same parameters. As shown in Fig. 5a, in the case of the thicker flux, in comparison with the conventional weld, the penetration of the weld decreased by about 22.3%, but the width of the weld increased by about 9.8%. This means that the flux acts as a barrier. The outward deviation of the weld was confirmed by the shape of the arc captured during welding (Fig. 5b). When the heat input increased by about 37 percent, a deep and narrow weld formed once again (Fig. 5c), even more than the thin flux. In this case, the shape of the arc was more focused (Fig. 5d), which agrees with the corresponding deeper weld. In higher heat input and flux thickness, perhaps a greater amount of the flux is decomposed, resulting in more oxygen entering the weld. Therefore, the enhancing mechanisms act more efficiently. Increasing heat input by the reduction in welding speed or increasing welding current leads to the higher efficiency of active fluxes [35].

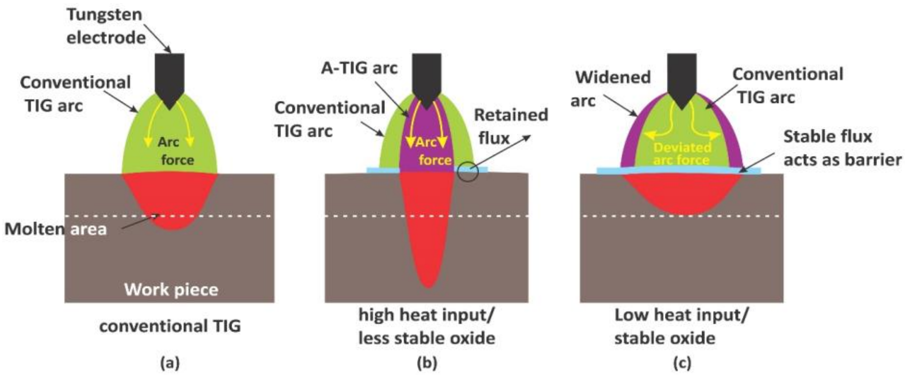

Fig. 4. Schematic representation of different mechanisms affecting penetration depth, a: conventional TIG, b: flux assisted TIG in high heat input process or less stable oxide fluxes, c: flux assisted TIG in low heat input process or stable oxide fluxes.

Comparing ferritic and austenitic steels with different thermo-physical properties helps to better understand the most contributing mechanisms in increasing weld penetration. Molten stainless steel has a higher viscosity than carbon steel [24]. The higher viscosity of austenitic steel was attributed to Ni alloying [36]. The surface tensions of austenitic and ferritic steels are almost the same [37]. Also, the melts of both alloys have nearly similar magnetic properties. Therefore, viscosity is the main difference between the melts of the two alloys in this study. However, this was not much discussed in the literature. A decrease in the melt viscosity would increase the weld penetration [25]. Moreover, dissolved oxygen could affect the viscosity and surface tension of the stainless steel considerably [26]. It could be argued that in the A-TIG process, if the weld penetration changes, especially in SS316, the mechanism in which the viscosity and surface tension are controlling parameters, i.e., the reversed Marangoni, could be the dominant mechanism. This disagrees with the works of Howse and Lucas [38] and Vasantharaja and Vasudevan [39] that propose arc constriction as the main penetration-enhancing mechanism.

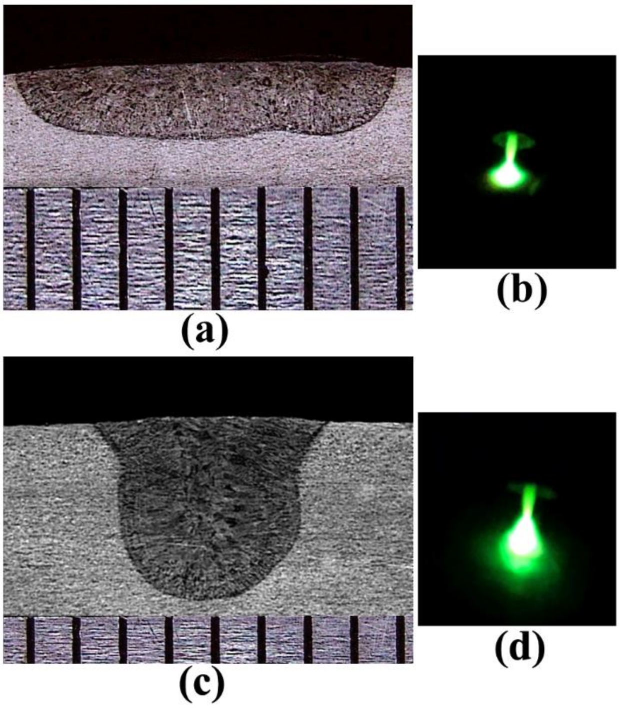

Fig. 5. Cross-sectional view and weld arc shape of the SS316 welds welded with a thick layer of MnO_2 flux a, b: low heat input (weld width: 7.6 mm, weld penetration 1.5 mm), c, d: high heat input (weld width: 4.7 mm, weld penetration 3.7 mm).

With regards to the smaller impact of oxide fluxes on A516 steel, it could be claimed that plain molten steel itself has low viscosity (less than 3.4 cP [40]), and the fluxes could not effectively reduce the surface tension of the weld in the welding temperature range [41]. Therefore, the mechanisms that increase penetration depth do not work effectively. This suggests that the decreasing mechanisms should act better, and finally, a reduction in the penetration takes place in the case of carbon steel. It is important to note that carbon steel has an inherent sulfur active agent, and oxide active fluxes could not activate or enhance the increasing mechanism. However, anyway, they could reduce the arc energy. In contrast, molten stainless steel has higher viscosity [42], and by adding oxygen, the increasing mechanism works more effectively, and finally, the penetration increases.

4. Conclusions

The present study was conducted to determine the dominant mechanism changing the geometry of the welds in the A-TIG welding of steels. The behaviors of ferritic and austenitic steel were evaluated using Al_2O_3, Fe_2O_3, MnO_2, SiO_2, and TiO_2 fluxes with different thermodynamical stabilities.

1- The oxide fluxes caused the penetration depth of the stainless steel welds to increase up to about 75 percent in the case of TiO_2, MnO_2 and Fe_2O_3. Al_2O_3 and SiO_2, with a respective 50 and 9 percent increase in the weld depth, were less effective.

2- In the case of carbon steel, the more stable oxides i.e., Al_2O_3 and SiO_2 had reversed effects and caused the depth of penetration to reduce by about 30 percent compared to that in conventional TIG welding. Oxides such as Fe_2O_3 could play a role in enhancing the penetration depth.

3- Based on the thermo-physical properties of carbon steel and stainless steel, it was decided that the penetration enhancement was mainly governed by the viscosity and surface tension, i.e., the reversed Marangoni rather than arc constriction was the dominating mechanism.

4- In active TIG, two mechanisms compete with each other: one increases the penetration, and the other one decreases the penetration. The former mechanism was well investigated in the literature, whereas the latter was completely ignored. The type and thickness of flux, i.e., the energy for flux decomposition and the barrier effect, are two parameters that consume and dissipate arc energy and reduce weld penetration.

5- When the heat input/arc energy is low, and a thick or stable flux exists, the second mechanism is dominant, and a reduction in the weld penetration results. But in high heat inputs and the presence of thin or less stable fluxes, the first mechanism dominates, and weld penetration increases. This has led researchers to obtain conflicting results in their investigations.

6- In alloys with higher viscosity and surface tension, like stainless steel, the first mechanism could be more effective. But contrariwise, in plain carbon steel with lower viscosity and surface tension, the enhancing mechanism's effect is insignificant, and the second mechanism could reduce the penetration and increase the weld width.

References

[1] G. Venkatesan, J. George, M. Sowmyasri, V. Muthupandi, "Effect of ternary fluxes on depth of penetration in A-TIG welding of aisi 409 ferritic stainless steel", Proc. Mat. Sci., Vol. 5, No. 2014, pp. 2402-2410.

[2] M. Muzamil, J. Wu, M. Akhtar, V. Patel, A. Majeed, J. Yang, "Multicomponent enabled MWCNTs-TiO2 nano-activating flux for controlling the geometrical behavior of modified TIG welding joint process", Diam. Relat. Mater., Vol. 97, No. 2019, pp. 107442.

[3] R. Vidyarthy, D.K. Dwivedi, "Activating flux tungsten inert gas welding for enhanced weld penetration", J. Manuf. Process., Vol. 22, No. 2016, pp. 211-228.

[4] D. Sharma, P.K. Ghosh, S. Kumar, S. Das, R. Anant, N. Kumar, "Surface hardening by in-situ grown composite layer on microalloyed steel employing TIG arcing process", Surf.Coat. Tech., Vol. 352, No. 2018, pp. 144-158.

[5] D. Li, S. Lu, W. Dong, D. Li, Y. Li, "Study of the law between the weld pool shape variations with the welding parameters under two TIG processes", J. Mater. Process. Tech., Vol. 212, No. 1, 2012, pp. 128-136.

[6] M. Mirzaei, A. Khodabandeh, H. Najafi, "Effect of active gas on weld shape and microstructure of highly efficient TIG welded A516 low carbon steel", T. Indian I. Metals, Vol. 69, No. 9, 2016, pp. 1723-1731.

[7] C. Heiple, P. Burgardt, "Effects of SO2 shielding gas additions on GTA weld shape", Weld. J., Vol. 64, No. 6, 1985, pp. 159-162.

[8] P. Burgardt, C. Heiple, "Interaction between impurities and welding variables in determining GTA weld shape", Weld. J., Vol. 65, No. 6, 1986, pp. 150.

[9] S. Pierce, P. Burgardt, D. Olson, "Thermocapillary and arc phenomena in stainless steel welding", Weld. J., Vol. 78, No. 1999, pp. 45-s.

[10] K.D. Ramkumar, A. Chandrasekhar, A.K. Singh, S. Ahuja, A. Agarwal, N. Arivazhagan, A.M. Rabel, "Comparative studies on the weldability, microstructure and tensile properties of autogeneous TIG welded AISI 430 ferritic stainless steel with and without flux", J. Manuf. Process., Vol. 20, No. 2015, pp. 54-69.

[11] S. Lu, H. Fujii, H. Sugiyama, M. Tanaka, K. Nogi, "Weld penetration and marangoni convection with oxide fluxes in GTA welding", Mater. Trans., Vol. 43, No. 11, 2002, pp. 2926-2931.

[12] K.A. Yushchenko, D.V. Kovalenko, I.V. Krivtsun, V.F. Demchenko, I.V. Kovalenko, A.B. Lesnoy, "Experimental studies and mathematical modelling of penetration in TIG and A-TIG stationary arc welding of stainless steel", Weld. World, Vol. 53, No. 9, 2009, pp. 253-263.

[13] G. Chandrasekar, C. Kailasanathan, D.K. Verma, K. Nandagopal, "Optimization of welding parameters, influence of activating flux and investigation on the mechanical and metallurgical properties of activated TIG weldments of AISI 316 L stainless steel", T. Indian I. Metals, Vol. 70, No. 3, 2017, pp. 671-684.

[14] G. Venkatesan, V. Muthupandi, J. Justine, "Activated TIG welding of AISI 304L using mono- and tri-component fluxes", Int. J. Adv. Manuf.Tech., Vol. 93, No. 1, 2017, pp. 329-336.

[15] H. Huang, S. Shyu, K. Tseng, C. Chou, "Evaluation of TIG flux welding on the characteristics of stainless steel", Sci. Technol. Weld. Join., Vol. 10, No. 5, 2005, pp. 566-573.

[16] S. Jayakrishnan, P. Chakravarthy, "Flux bounded tungsten inert gas welding for enhanced weld performance—a review", J. Manuf. Process., Vol. 28, No. 2017, pp. 116-130.

[17] A. Berthier, P. Paillard, M. Carin, F. Valensi, S. Pellerin, "TIG and A-TIG welding experimental investigations and comparison to simulation: Part 1: Identification of marangoni effect", Sci. Technol. Weld. Join., Vol. 17, No. 8, 2012, pp. 609-615.

[18] N.P. Patel, V.J. Badheka, J.J. Vora, G.H. Upadhyay, "Effect of oxide fluxes in activated TIG welding of stainless steel 316LN to low activation

ferritic/martensitic steel (LAFM) dissimilar combination", T. Indian I. Metals, Vol. 72, No. 10, 2019, pp. 2753-2761.
[19] J.J. Vora, V.J. Badheka, "Improved penetration with the use of oxide fluxes in activated TIG welding of low activation ferritic/martensitic steel", T. Indian I. Metals, Vol. 69, No. 9, 2016, pp. 1755-1764.
[20] A.G. Luciano de Azevedo, V.A. Ferraresi, J.P. Farias, "Ferritic stainless steel welding with the A-TIG process", Weld. Int., Vol. 24, No. 8, 2010, pp. 571-578.
[21] K.-H. Tseng, C.-Y. Hsu, "Performance of activated TIG process in austenitic stainless steel welds", J. Mater. Process. Tech., Vol. 211, No. 3, 2011, pp. 503-512.
[22] G.-h. Liu, M.-h. Liu, Y.-y. Yi, Y.-p. Zhang, Z.-y. Luo, L. Xu, "Activated flux tungsten inert gas welding of 8 mm-thick AISI 304 austenitic stainless steel", J. Cent. South Univ., Vol. 22, No. 3, 2015, pp. 800-805.
[23] K.H. Dhandha, V.J. Badheka, "Effect of activating fluxes on weld bead morphology of P91 steel bead-on-plate welds by flux assisted tungsten inert gas welding process", J. Manuf. Process., Vol. 17, No. 2015, pp. 48-57.
[24] J.J. Valencia, P.N. Quested, "Thermophysical properties", 2013.
[25] B. Pollard, "The effects of minor elements on the welding characteristics of stainless steel", Weld. J., Vol. 67, No. 9, 1988, pp. 202s-213s.
[26] D. Aidun, S. Martin, "Effect of sulfur and oxygen on weld penetration of high-purity austenitic stainless steels", J. Mater. Eng. Perform., Vol. 6, No. 4, 1997, pp. 496-502.
[27] P. Marashi, M. Pouranvari, S. Amirabdollahian, A. Abedi, M. Goodarzi, "Microstructure and failure behavior of dissimilar resistance spot welds between low carbon galvanized and austenitic stainless steels", Mater. Sci. Eng., Vol. 480, No. 2008, pp. 175-180.
[28] P. Kumar, A.N. Sinha, "Effect of pulse width in pulsed ND: YAG dissimilar laser welding of austenitic stainless steel (304 L) and carbon steel (st37)", Lasers Manuf. Mater., Vol. 5, No. 4, 2018, pp. 317-334.
[29] M.H. Bina, M. Jamali, M. Shamanian, H. Sabet, "Investigation on the resistance spot-welded austenitic/ferritic stainless steel", Int. J. Adv. Manuf.Tech., Vol. 75, No. 9, 2014, pp. 1371-1379.
[30] M. Abbaoui, B. Cheminat, P. Andanson, "Influence of the nature of the metal on the conductivity of an argon-metal plasma", J. Phys. D Appl. Phys., Vol. 18, No. 10, 1985, pp. L159.
[31] S. Mishra, T. Lienert, M. Johnson, T. DebRoy, "An experimental and theoretical study of gas tungsten arc welding of stainless steel plates with different sulfur concentrations", Acta Mater., Vol. 56, No. 9, 2008, pp. 2133-2146.
[32] S. Lu, H. Fujii, H. Sugiyama, M. Tanaka, K. Nogi, "Effects of oxygen additions to argon shielding gas on GTA weld shape", ISIJ int., Vol. 43, No. 10, 2003, pp. 1590-1595.
[33] S.H. Elahi, H. Abdi, H. Shahverdi, "Investigating viscosity variations of molten aluminum by calcium addition and stirring", Mater. Lett., Vol. 91, No. 2013, pp. 376-378.
[34] S.H. Elahi, H. Abdi, H. Shahverdi, "A new method for investigating oxidation behavior of liquid metals", Rev. Sci. Instrum., Vol. 85, No. 1, 2014, pp. 015115.
[35] H. Fujii, T. Sato, S. Lu, K. Nogi, "Development of an advanced A-TIG (AA-TIG) welding method by control of marangoni convection", Mater. Sci. Eng. A, Vol. 495, No. 1-2, 2008, pp. 296-303.
[36] L. Pilcher, "Welding dissimilar metals ", 2015.
[37] R. Brooks, P. Quested, "The surface tension of steels", J. Mater. Sci., Vol. 40, No. 9, 2005, pp. 2233-2238.
[38] D. Howse, W. Lucas, "Investigation into arc constriction by active fluxes for tungsten inert gas welding", Sci. Technol. Weld. Join., Vol. 5, No. 3, 2000, pp. 189-193.
[39] P. Vasantharaja, M. Vasudevan, "Studies on A-TIG welding of low activation ferritic/martensitic (LAFM) steel", J.Nucl. Mater., Vol. 421, No. 1-3, 2012, pp. 117-123.
[40] M. Rywotycki, Z. Malinowski, J. Giełżecki, A. Gołdasz, "Modelling liquid steel motion caused by electromagnetic stirring in continuous casting steel process", Arch. Metall. Mater., Vol. 59, No. 2, 2014, pp. 487--492.
[41] K. Morohoshi, M. Uchikoshi, M. Isshiki, H. Fukuyama, "Surface tension of liquid iron as functions of oxygen activity and temperature", ISIJ int., Vol. 51, No. 10, 2011, pp. 1580-1586.
[42] J. Zhou, H.-L. Tsai, T. Lehnhoff, "Investigation of transport phenomena and defect formation in pulsed laser keyhole welding of zinc-coated steels", J. Phys. D Appl. Phys., Vol. 39, No. 24, 2006, pp. 5338.